Microscopic analysis of quadrupole collective motion in Cr-Fe nuclei. I. Renormalization of collective states and interacting boson model parameters

Hitoshi Nakada
Department of Physics, Faculty of Science, Chiba University, Yayoi-cho 1-33, Inage-ku, Chiba 263, Japan

Takaharu Otsuka
Department of Physics, Faculty of Science, University of Tokyo, Hongo 7-3-1, Bunkyo-ku, Tokyo 113, Japan
(Received 30 September 1996)

We present a new method by which wave functions with simple structure are renormalized so as to contain more complicated structure. This method, called H^n-cooling method, is applied to the study of the quadrupole collective motion of ^{56}Fe, ^{54}Cr, ^{58}Fe, and ^{56}Cr. The shell-model wave functions of lowest-lying states of these nuclei are well treated by this method. By using the wave functions obtained via the H^n-cooling method, interacting boson model-2 parameters are derived from a realistic shell-model Hamiltonian and transition operators. The Majorana interaction becomes sizably repulsive, primarily as an effect of the renormalization. The bosonic $E2$ effective charges are enhanced due to the renormalization, while a quenching occurs in the $M1$ and $M3$ parameters for proton bosons. It is shown that the χ parameters take similar values in the Hamiltonian and in the $E2$ operator. [S0556-2813(97)05902-5]

PACS number(s): 21.10.Re, 21.60.Cs, 21.60.Ev, 27.40.+z

I. INTRODUCTION

Middle pf-shell nuclei provide us with a precious testing ground to understand various aspects of the quadrupole collective motion from microscopic standpoints. Computational difficulties in a realistic shell model rise rapidly in general, as the mass number increases. The growing computer power, however, enables us to carry out realistic shell-model calculations in the middle pf-shell region. On the other side, the middle pf-shell nuclei seem to gain significant quadrupole collectivity, which is a global and dominating feature of heavier nuclei.

Recently we have reported one of the most successful shell-model results for $N=28$–30 nuclei [1–3]. The Kuo-Brown interaction [4], which had been derived from a realistic NN potential through G matrix, has been employed in these calculations, together with a large configuration space including excitations from the $0f_{7/2}$ orbit. To be more precise, considering the following configuration:

$$(0f_{7/2})^{n_1-k}(0f_{5/2}1p_{3/2}1p_{1/2})^{n_2+k}, \tag{1}$$

where $n_1=(Z-20)+8$ and $n_2=N-28$ for the $20<Z\leqslant 28 \leqslant N<40$ nuclei, we have adopted a space consisting of all the $k=0$, 1, and 2 configurations. It has been confirmed [3] that, for even-even nuclei, the energy levels are reproduced remarkably well for $E_x<4$ MeV.

The presence of mixed-symmetry states with respect to the proton and neutron collective degrees of freedom has been predicted by the proton-neutron interacting boson model (IBM-2) [5]. It has been pointed out [6] that a mixed-symmetry 2^+ state may lie lower than the other mixed-symmetry states in spherical nuclei, although the origin of such a low-lying mixed-symmetry 2^+ level has remained open. Experimental studies have suggested that the mixed-symmetry 2^+ state exists around $E_x=3$ MeV in the Cr-Fe region [7]. A realistic shell-model analysis has been applied to pin down the mixed-symmetry 2^+ state of ^{56}Fe [1], clarifying which states share substantial fractions of the mixed-symmetry component. It is of special interest to study this type of collective mode more extensively, on the basis of a realistic shell-model calculation.

The realistic shell-model Hamiltonian couples collective degrees of freedom to non-collective ones, in general. When large-scale shell-model results are interpreted in terms of IBM-2, it is important to incorporate, through a certain renormalization procedure, effects of relevant noncollective degrees of freedom into the calculations made in the collective subspace. This is an example of the general problem as to how a complicated system can be described with a limited number of degrees of freedom by taking into account a variety of correlations in an effective manner. Rayleigh-Schrödinger's perturbation theory constitutes a possible way, by which the model wave function is modified. The second-order perturbation has been applied to renormalize the IBM-2 parameters [8,9]. Another way is Bloch-Horowitz's renormalization of operators, in which operators, rather than wave functions, are modified perturbatively so as to carry the relevant correlation effects. Some useful general theories have been developed by extending Bloch-Horowitz's method: Feshbach's projection method [10] and the folded-diagram theory [11], for example. These methods are, however, more or less based on the perturbation theory. In the cases to be considered in this paper, perturbative ways are inappropriate, as is argued just below.

Our present goal is an investigation of the quadrupole collective states which are to be described within IBM-2, in connection with the realistic shell model. In the first approximation, the s and d bosons in IBM-2 correspond to the collective 0^+ (S) and 2^+ (D) pairs of valencelike nucleons [5]. In Cr-Fe nuclei, as is assumed in Ref. [7], the S and D pairs normally comprise only the $k=0$ configuration of Eq. (1), because of the $Z=N=28$ magic number. The realistic shell-

 © 1997 The American Physical Society

model wave functions, however, contain other configurations. According to the realistic shell-model results, the leakage out of the $k=0$ space is so significant that even the 0_1^+ and 2_1^+ wave functions are not well enough covered with this usual SD space ($<60\%$) [3]. In order that the 0_1^+ and 2_1^+ states can be described within the IBM-2, the correlations beyond the SD pairs must be taken into account. This relatively large $k>0$ fraction prevents perturbative ways from being applicable. A method beyond the perturbation theory is required. It is commented that this situation takes place because the ^{56}Ni core is not very stiff. Perturbative approaches may be legitimate in other mass regions in connecting IBM-2 to realistic shell model.

We recall here that, as far as several lowest-lying levels are concerned, they are successfully reproduced by the Horie-Ogawa Hamiltonian [12] with only the $k=0$ configuration in the Cr-Fe region, apart from the precise description of the mixed-symmetry states [1]. Moreover, this $k=0$ shell-model result is connected with IBM-2 fairly well, at least for 0_1^+ and 2_1^+ [13]. This fact suggests that, even in more realistic cases with $k>0$ configurations, the lowest-lying states may be described within IBM-2 through a proper renormalization. In Ref. [1] modified SD pairs have been introduced, and the fragmentation of the mixed-symmetry 2^+ components was clarified for ^{56}Fe.

We introduce a new and yet simple method in this article. It is applicable even to some cases where the perturbation does not work well. The method is applied to quadrupole collective states of Cr-Fe nuclei, and the wave functions of those states are renormalized. In addition to ^{56}Fe and ^{54}Cr, on which the shell-model results have already been reported in Ref. [3], ^{58}Fe and ^{56}Cr are studied. Furthermore, by extending the OAI mapping [5], the IBM-2 Hamiltonian is derived from the realistic shell-model Hamiltonian. This is the first work of this sort, while there have been many works evaluating IBM-2 parameters from more schematic interactions, for instance the surface-delta interaction. The IBM-2 transition operators are obtained as well. Renormalization effects on various IBM-2 parameters are discussed. Focusing on the IBM-2 results more concisely, we shall investigate properties of the mixed-symmetry states in Cr-Fe region in the following paper [14].

II. H^n-COOLING METHOD (H^nCM)

The present renormalization method is introduced in a general form, in this section. Some details of the procedure will be illustrated in Sec. III. Although this method may be applicable to other many-body problems, we shall apply it, in this paper, to elicit a collective space out of the shell-model space. This collective space should correspond to that of IBM-2.

In ^{56}Fe, for example, we have a pair of proton holes and a pair of valence neutrons within the description assuming the ^{56}Ni core. The S and D pairs of protons are defined as the 0^+ and 2^+ states of the $(0f_{7/2})^{-2}$ configuration, while those of neutrons are collective 0^+ and 2^+ states of the $(0f_{5/2}1p_{3/2}1p_{1/2})^2$ configuration. Once the structure of the neutron S and D pairs is given, the SD space is constructed by these proton and neutron S and D pairs.

We first introduce a subspace of the original Hilbert space. This subspace is denoted by $W^{(0)}$. In the application discussed in Sec. IV, the original space corresponds to the shell-model space, and $W^{(0)}$ to the SD space. The bases belonging to $W^{(0)}$ are hereafter called *primary* bases, while those outside $W^{(0)}$ *nonprimary* bases. It is required that the primary bases include basic dynamics already. If there is a conserved quantum number J, the space $W^{(0)}$ can be decomposed as

$$W^{(0)}=\oplus_J W_J^{(0)}. \tag{2}$$

In the practical case, J represents nuclear spin. In the following procedure, $W_J^{(0)}$'s with different J's never mix with one another, reflecting the conservation law.

We consider a primary basis $\Psi_\lambda^{(0)}\in W_J^{(0)}$ where λ is the index of basis-state vectors for a given J. The quantum number J is not explicitly shown in $\Psi_\lambda^{(0)}$ for brevity. The state $\Psi_\lambda^{(0)}$ evolves with time t as $e^{-iHt}|\Psi_\lambda^{(0)}\rangle$, where H means the original Hamiltonian. When the inverse temperature $\beta=it$ with imaginary t is employed, the time evolution e^{-iHt} is converted to cooling $e^{-\beta H}$. In order to simplify the following discussion, we assume without loss of generality that all the eigenenergies are non-negative. This situation is attained, if necessary, by shifting the origin of energy. The expectation value $\langle\Psi_\lambda^{(0)}|e^{-\beta H}|\Psi_\lambda^{(0)}\rangle$, which is a function of β, is a superposition of exponentially-decreasing components corresponding to eigenvalues of H. The number of these components is much larger, in general, than the dimension of $W^{(0)}$, because a sizable fraction of $e^{-\beta H}|\Psi_\lambda^{(0)}\rangle$ escapes out of $W^{(0)}$ with increasing β; $e^{-\beta H}W_J^{(0)}\neq W_J^{(0)}$ and therefore $e^{-\beta H}W^{(0)}\neq W^{(0)}$. We consider, in this paper, the situations in which the primary bases form a major part of some low-lying states and then $\langle\Psi_\lambda^{(0)}|e^{-\beta H}|\Psi_\lambda^{(0)}\rangle$ is dominated by one or a few slowly decreasing components, while fast-decaying components are superposed with far smaller amplitudes. If we choose appropriate states from nonprimary bases, only a small number of them will have a sizable mixing with $\Psi_\lambda^{(0)}$. These nonprimary but relevant bases are here expressed as $\phi_\lambda^{(\nu)}$. The superscript (ν) is used as an index of degree of the coupling to $\Psi_\lambda^{(0)}$, whose meaning will be specified later in this section. By taking into account the influence of the ϕ bases, the wave function of $\Psi_\lambda^{(0)}$ will be renormalized as

$$\Psi_\lambda\propto\Psi_\lambda^{(0)}+\sum_\nu c_{\nu,\lambda}\phi_\lambda^{(\nu)}, \tag{3}$$

where $c_{\nu,\lambda}$ represents mixing amplitude of the ϕ basis. The basis Ψ_λ is constructed so as to contain higher-energy components with significantly small amplitudes. By doing this, rapidly decreasing components in $\langle\Psi_\lambda|e^{-\beta H}|\Psi_\lambda\rangle$ can be made negligibly small. Then the exact low-lying eigenstates will be reproduced to a good approximation by appropriate linear combinations of Ψ_λ's. The following discussion will exhibit how to choose $\phi_\lambda^{(\nu)}$ efficiently and how to evaluate $c_{\nu,\lambda}$. With an adequate set of $\phi_\lambda^{(\nu)}$'s and $c_{\nu,\lambda}$'s, the truncation up to relatively small ν in Eq. (3) is expected to yield good renormalized bases, as will be shown with concrete examples.

In the present method, it is required that the Hilbert space $W_J \equiv \{\Psi_\lambda ; \lambda = 1,2, \ldots\}$, which consists of the renormalized bases, fulfills the approximate relation

$$e^{-\beta H} W_J \approx W_J , \tag{4}$$

up to a reasonably large β. By defining the total space of the renormalized bases by

$$W \equiv \oplus_J W_J , \tag{5}$$

Eq. (4) can be expressed as

$$e^{-\beta H} W \approx W. \tag{6}$$

We look for a W which satisfies Eq. (6) and, at the same time, remains a rather small subspace of the full Hilbert space. Equation (4) or Eq. (6) indicates approximate closure of the renormalized space. The closure is exactly satisfied if W consists of eigenstates of H. Such a construction, however, only means a calculation in the full space. We are here seeking to obtain W_J with a limited number of the ϕ bases in Eq. (3), discarding degrees of freedom coupled to the primary bases only weakly. For this purpose, we shall trace how the original basis $\Psi_\lambda^{(0)}$ evolves by $e^{-\beta H}$.

We consider a small β by rewriting β as $\Delta\beta$ for the time being, although it is not essential as discussed later. By expanding $e^{-\Delta\beta H}$ into the power series of $\Delta\beta$, the cooling of $\Psi_\lambda^{(0)}$ gives

$$e^{-\Delta\beta H} |\Psi_\lambda^{(0)}\rangle = \left[\sum_{\nu=0}^{n} \frac{(-\Delta\beta)^\nu}{\nu!} H^\nu + \hat{O}((\Delta\beta)^{n+1}) \right] |\Psi_\lambda^{(0)}\rangle, \tag{7}$$

where $\hat{O}((\Delta\beta)^\nu)$ represents an operator with the order of $(\Delta\beta)^\nu$. We define the $\phi_\lambda^{(\nu)}$ bases [see Eq. (3)] from the right-hand side,

$$|\phi_\lambda^{(\nu)}\rangle \equiv P^{\mathcal{O}} \cdot H^\nu |\Psi_\lambda^{(0)}\rangle. \tag{8}$$

Here $P^{\mathcal{O}}$ stands for an appropriate orthonormalization, whose concrete definition will be given in Sec. III. The basis $\phi_\lambda^{(1)}$ directly couples to $\Psi_\lambda^{(0)}$ via H, exhausting the coupling leading out of $W_J^{(0)}$. The next basis $\phi_\lambda^{(2)}$ affects the primary state via its coupling to $\phi_\lambda^{(1)}$. In this manner, important bases are extracted one after another. Note that all the ϕ bases carry the same quantum number J as $\Psi_\lambda^{(0)}$.

Since the shell model is defined as a finite dimensional many-body problem, the cooling operator $e^{-\Delta\beta H}$ does not need infinite series expansion. Moreover, since we have postulated that the primary bases include basic dynamics, the number of relevant degrees of freedom which couple to the primary bases can be relatively small. Making good use of these features, $e^{-\Delta\beta H}$ is handled by the power-series expansion as in Eq. (7), and the ϕ bases are generated by Eq. (8).

It has been known that the Lanczos diagonalization algorithm is efficient to obtain eigenenergies and eigenfunctions of low-lying states. We here try to utilize the advantage of the Lanczos method. The Lanczos method can be derived via the power-series expansion of $e^{-\Delta\beta H}$ acting on an arbitrary basis. Besides a difference in the $P^{\mathcal{O}}$ operator (see Sec. III), the ϕ bases in Eq. (8) have basically the same form as the Lanczos bases generated from $\Psi_\lambda^{(0)}$. However, it is a key point of the present method that the primary bases contain basic dynamics of the system. In other words, the primary bases form the main part of the wave functions of the low-lying states under interest. Thereby we can regard the current procedure as a renormalization. The relation of the present method to the Lanczos method will be discussed further in Sec. VI.

Let us begin with a simple case in which there is just a single state $\Psi^{(0)}$ in $W_J^{(0)}$. We do not need the label λ in this case. The $P^{\mathcal{O}}$ operator in Eq. (8) expresses the Gram-Schmidt orthogonalization to $\Psi^{(0)}$ and $\phi^{(\nu')}$'s with $\nu' < \nu$. We thus generate a subspace $\Gamma^{(n)} \equiv \{\Psi^{(0)}, \phi^{(1)}, \phi^{(2)}, \ldots, \phi^{(n)}\}$, corresponding to the order of $(\Delta\beta)^n$.

A renormalized wave function [see Eq. (3)] is introduced within $\Gamma^{(n)}$,

$$\Psi^{(n)} \propto \Psi^{(0)} + \sum_{\nu=1}^{n} c_\nu \phi^{(\nu)}, \tag{9}$$

with the amplitude c_ν's to be determined. The submatrix of H for the subspace $\Gamma^{(n)}$ is constructed, and the eigenvector associated with the lowest eigenvalue is adopted as the renormalized basis $\Psi^{(n)}$ in Eq. (9). It is noticed that the mixing amplitude c_ν thus obtained depends on n, though this dependence is not explicitly shown here. The basis $\Psi^{(n)}$ yields

$$e^{-\Delta\beta H} |\Psi^{(n)}\rangle = e^{-\Delta\beta E^{(n)}} |\Psi^{(n)}\rangle + [\hat{O}((\Delta\beta)^{n+1})] |\Psi^{(0)}\rangle, \tag{10}$$

where $E^{(n)} = \langle\Psi^{(n)}|H|\Psi^{(n)}\rangle$. By this procedure, rapidly decreasing components become substantially smaller in $\langle\Psi^{(n)}|e^{-\Delta\beta H}|\Psi^{(n)}\rangle$ than in $\langle\Psi^{(0)}|e^{-\Delta\beta H}|\Psi^{(0)}\rangle$. The $\Psi^{(0)}$ state is thus cooled down. Increasing n step by step, we can monitor what components are adopted in higher-order steps.

When we have $l(>1)$ bases in $W_J^{(0)}$, the renormalized basis $\Psi_\lambda^{(n)}$ is obtained for each λ by diagonalizing a submatrix of H in $\Gamma_\lambda^{(n)}$, which is generated from $\Psi_\lambda^{(0)}$. The $\Psi_\lambda^{(n)}$ $(\lambda = 1, \cdots, l)$ bases span a space $W_J^{(n)}$. However, H may produce crossover couplings among bases in $\Gamma_\lambda^{(n)}$ with different λ, which gives rise to a nonorthogonality between bases with different λ. In order to avoid this, $\Gamma_\lambda^{(n)}$ is created so as to be orthogonal to $\Gamma_{\lambda'}^{(n)}$ if $\lambda \neq \lambda'$, by carrying out an orthonormalization. This orthogonalization will be illustrated concretely in Sec. III. Although this modification can generally break the relation (10) for individual basis, the orthonormalization can be made (see Sec. III) so that a similar condition should be satisfied for the space $W_J^{(n)}$,

$$e^{-\Delta\beta H} W_J^{(n)} = W_J^{(n)} + [\hat{O}((\Delta\beta)^{n+1})] W_J^{(0)}. \tag{11}$$

This indicates that $W_J^{(n)}$ fulfills Eq. (4) up to $O((\Delta\beta)^n)$. The entire space of the renormalized space at the order n is then defined as

$$W^{(n)} \equiv \oplus_J W_J^{(n)}. \tag{12}$$

The cooling Eq. (11) is carried out step by step, through the power-series expansion (7). We shall call the present procedure H^n-cooling method (H^nCM). The H^nCM gives a wave function renormalization, incorporating dynamical correlations contained in H. As far as the H^1CM is concerned, the state $e^{-\beta H}|\Psi_\lambda^{(0)}\rangle$ with small β is decomposed in terms of the $n=1$ basis $\Psi_\lambda^{(1)}$ and the rest. The latter has higher energy than the former, giving rise to the faster-decreasing component. Analogously, for a general n, the H^nCM process produces n faster-decreasing components in addition to the slowest-decreasing component (i.e., $\Psi_\lambda^{(n)}$). The closure of the renormalized subspace $W^{(n)}$ is fulfilled up to $O((\Delta\beta)^n)$, as is shown in Eq. (11). The larger n assures the better approximation from the viewpoint of the condition (4) or (6). If $W^{(n)}$ converges with n, no new basis is created by H acting on this subspace. The convergence then becomes independent of β, which means that Eq. (6) holds for a general value of β, not only for $\Delta\beta$.

Although a cooling can be made only by operating $e^{-\Delta\beta H}$ on $\Psi_\lambda^{(0)}$, in the H^nCM the diagonalization is performed within $\Gamma_\lambda^{(n)}$ for each step. This accelerates the cooling to an appreciable extent, since the diagonalization is equivalent to the full cooling within the relevant subspace. Moreover, as far as the dimension of H is finite, bases are exhausted at finite n. Therefore, the $\beta\to\infty$ limit, which is required for the full cooling in infinite-dimensional cases, is not necessary. Because of these properties, all the major components for low-lying states are generated with relatively small β, and the H^nCM is expected to be efficient even with rather small n. We shall see it in practice in Sec. IV.

Here we should add the comment that some nuclear collective states, for which the H^nCM will be used, are not necessarily the lowest-lying state with a specific spin-parity. In such cases the term ''cooling'' may not be appropriate, and some caution will be necessary in applying the present method. A prescription will be shown in Sec. VI, while the actual case of the Cr-Fe nuclei will be presented in Ref. [14].

III. ILLUSTRATION OF H^nCM

The H^nCM is illustrated in some detail with an example: let us consider the set spanned by the SD states with $J^P=2^+$ in ^{56}Fe.

As has been mentioned in the preceding section, the proton S and D pairs have the $(0f_{7/2})^{-2}$ configuration in ^{56}Fe, while the neutron pairs have the $(0f_{5/2}1p_{3/2}1p_{1/2})^2$ configuration. The set of 2^+ states within this SD space of ^{56}Fe comprises the following bases:

$$|2^+(SD);F=1\rangle=\frac{1}{\sqrt{2}}(|D_\pi\rangle\otimes|S_\nu\rangle+|S_\pi\rangle\otimes|D_\nu\rangle), \quad (13a)$$

$$|2^+(D^2);F=1\rangle=[|D_\pi\rangle\otimes|D_\nu\rangle]^{(2)}, \quad (13b)$$

$$|2^+(SD);F=0\rangle=\frac{1}{\sqrt{2}}(|D_\pi\rangle\otimes|S_\nu\rangle-|S_\pi\rangle\otimes|D_\nu\rangle). \quad (13c)$$

These bases straightforwardly correspond to the IBM-2 bases through the OAI mapping [5]. In the following discussions, the proton-neutron property of the wave functions is taken into consideration, so that the states should correspond to the IBM-2 states with good F spin. The variable F on the left-hand side of Eq. (13) indicates the F-spin value of the corresponding IBM basis after the OAI mapping [5]. The maximum of F is obtained by $F_{\max}=\frac{1}{2}N^{\mathrm{B}}$, where $N^{\mathrm{B}}=N_\pi^{\mathrm{B}}+N_\nu^{\mathrm{B}}$ is the total number of SD pairs, which is the same as the total boson number in the IBM-2, for each nucleus. The states with $F=F_{\max}$ are called totally symmetric states in the IBM-2, while those with $F=F_{\max}-1$ mixed-symmetry states. We refer here the bases in the SD fermion space in an analogous manner. Note that $F_{\max}=1$ in ^{56}Fe. Though the above $|2^+(SD);F=0\rangle$ state is a totally anti-symmetric state, it is called mixed-symmetry state in this article because it belongs to the class of the $F=F_{\max}-1$ states.

For each nucleus we shall consider the complete set of orthonormal bases belonging to $W_J^{(0)}$ (i.e., the SD space with a specific spin); $\Psi_1^{(0)}$, $\Psi_2^{(0)}$, . . . , $\Psi_l^{(0)}$. In the above case of Eq. (13), the $\Psi^{(0)}$'s turn out to be

$$|\Psi_1^{(0)}\rangle=|2^+(SD);F=1\rangle, \quad |\Psi_2^{(0)}\rangle=|2^+(D^2);F=1\rangle,$$

$$|\Psi_3^{(0)}\rangle=|2^+(SD);F=0\rangle. \quad (14)$$

The ordering of the bases may affect the process of the H^nCM, as will become transparent below. In this example, the SD bases are ordered so that the class of states with full F-spin symmetry ($F=F_{\max}$) should come first, those with next highest F spin ($F=F_{\max}-1$) come second, and so forth. Within each sector of a given F spin, the bases are placed from the lower seniority to the higher, similarly to the OAI mapping.

In the H^nCM, the ϕ bases of Eq. (8) as well as the $\Psi^{(0)}$'s are generated in the following order:

$$\begin{gathered}\Psi_1^{(0)},\Psi_2^{(0)},\ldots,\Psi_l^{(0)},\\ \phi_1^{(1)},\phi_2^{(1)},\ldots,\phi_l^{(1)},\\ \phi_1^{(2)},\phi_2^{(2)},\ldots,\phi_l^{(2)},\\ \cdots\cdots\cdots,\\ \phi_1^{(n)},\phi_2^{(n)},\ldots,\phi_l^{(n)}.\end{gathered} \quad (15)$$

Recall that $\phi_\lambda^{(\nu)}$ is generated from $H^\nu\Psi_\lambda^{(0)}$, apart from the orthonormalization by $P^{\mathcal{O}}$. We define the $P^{\mathcal{O}}$ operator in Eq. (8) as follows. The first l bases are $\Psi_1^{(0)}$, $\Psi_2^{(0)}$, . . . , $\Psi_l^{(0)}$, which are already orthonormal, and $P^{\mathcal{O}}$ acts as the unity for them. The $(l+1)$th basis is $\phi_1^{(1)}$ generated from $H\Psi_1^{(0)}$ with the Gram-Schmidt orthogonalization to $\Psi_1^{(0)}$, $\Psi_2^{(0)}$, . . . , $\Psi_l^{(0)}$. Namely,

$$\phi_1^{(1)}\equiv P^{\mathcal{O}}_{\{\Psi_1^{(0)},\ldots,\Psi_l^{(0)}\}}\cdot H\Psi_1^{(0)}, \quad (16)$$

where $P^{\mathcal{O}}_{\{\}}$ represents orthogonalization to the states specified in the curly bracket, together with the normalization. The $(l+2)$th basis $\phi_2^{(1)}$ is created similarly, except that it should be orthogonal also to $\phi_1^{(1)}$,

$$\phi_2^{(1)} \equiv P^{\mathcal{O}}_{\{\Psi_1^{(0)},\ldots,\Psi_l^{(0)},\phi_1^{(1)}\}} \cdot H\Psi_2^{(0)}. \tag{17}$$

One can repeat the procedure until all the orthonormal bases in Eq. (15) are obtained. Each ϕ basis can be represented explicitly as

$$\phi_\lambda^{(\nu)} \equiv P^{\mathcal{O}}_{\{\Psi_1^{(0)},\ldots,\Psi_l^{(0)},\phi_1^{(1)},\ldots,\phi_l^{(\nu-1)}\}} \cdot H^\nu \Psi_\lambda^{(0)} \quad (\text{for } \lambda=1), \tag{18a}$$

$$\phi_\lambda^{(\nu)} \equiv P^{\mathcal{O}}_{\{\Psi_1^{(0)},\ldots,\Psi_l^{(0)},\phi_1^{(1)},\ldots,\phi_l^{(\nu-1)},\phi_1^{(\nu)},\ldots,\phi_{\lambda-1}^{(\nu)}\}} \cdot H^\nu \Psi_\lambda^{(0)} \quad (\text{for } \lambda\neq 1). \tag{18b}$$

Note that, as n becomes larger, some bases may vanish due to the orthogonalization. The bases in Eq. (15) are produced in this manner, by carrying out the Gram-Schmidt orthogonalization on them successively.

We then consider a subset $\Gamma_\lambda^{(n)} \equiv \{\Psi_\lambda^{(0)}, \phi_\lambda^{(1)}, \phi_\lambda^{(2)}, \ldots, \phi_\lambda^{(n)}\}$ for each $\lambda(=1,2,\ldots,l)$. It should be noticed that $\Gamma_\lambda^{(n)}$ is spanned by the bases constituting the λth column of Eq. (15). In order to obtain a renormalized basis $\Psi_\lambda^{(n)}$ [i.e., to evaluate $c_{\nu,\lambda}$ of Eq. (3)], we construct a submatrix of H within this subspace $\Gamma_\lambda^{(n)}$. After diagonalizing this submatrix, the lowest eigenstate is taken as the λth basis in $W_J^{(n)}$. In this manner, $\Psi_\lambda^{(1)}$ is obtained from $\Gamma_\lambda^{(1)} = \{\Psi_\lambda^{(0)}, \phi_\lambda^{(1)}\}$, $\Psi_\lambda^{(2)}$ from $\Gamma_\lambda^{(2)} = \{\Psi_\lambda^{(0)}, \phi_\lambda^{(1)}, \phi_\lambda^{(2)}\}$, and so forth. The H^{n}CM space $W^{(n)}$ is spanned by the bases thus obtained.

The H^{n}CM will be useful for extracting some simple structural features from complicated shell-model wave functions. Since the renormalized wave functions of the *SD* states are explicitly constructed, it is possible to compare them directly to the shell-model wave functions. It is also straightforward to evaluate matrix elements of a given operator in the space $W^{(n)}$. Although the larger n implies the better closure of the subspace from the viewpoint of Eq. (4), we consider $n\leqslant 2$ cases in the following application.

IV. APPLICATION OF H^{n}CM TO *SD* SPACE IN Cr-Fe NUCLEI

The H^{n}CM is applied and tested numerically in Cr-Fe nuclei, starting from the *SD*-pair states.

As has been shown in Ref. [3], the shell-model calculation with the Kuo-Brown realistic Hamiltonian in the $k\leqslant 2$ space successfully reproduces the observed states up to $E_x \simeq 4$ MeV in ^{54}Cr and ^{56}Fe. While the proton S and D pairs are uniquely determined by the $(0f_{7/2})^{-2}$ configuration, the structure of the neutron pairs has to be fixed. In ^{56}Fe, the structure of $|S_\nu\rangle$ is determined so as to maximize the overlap between the $|S_\pi\rangle\otimes|S_\nu\rangle$ state and the shell-model 0_1^+ state. The structure of $|D_\nu\rangle$ is determined so that the overlap between $|S_\pi\rangle\otimes|D_\nu\rangle$ and the shell-model 2_1^+ state should be maximum. The neutron pair structure for ^{54}Cr is fixed so as for $|S_\pi^2\rangle\otimes|S_\nu\rangle$ ($|S_\pi^2\rangle\otimes|D_\nu\rangle$) to have maximum overlap with the shell-model 0_1^+ (2_1^+) state. The structure of neutron pairs is slightly different between ^{56}Fe and ^{54}Cr. Note that the seniority projection [5] is carried out when $|D_\pi^2;J\rangle$ is produced in Cr.

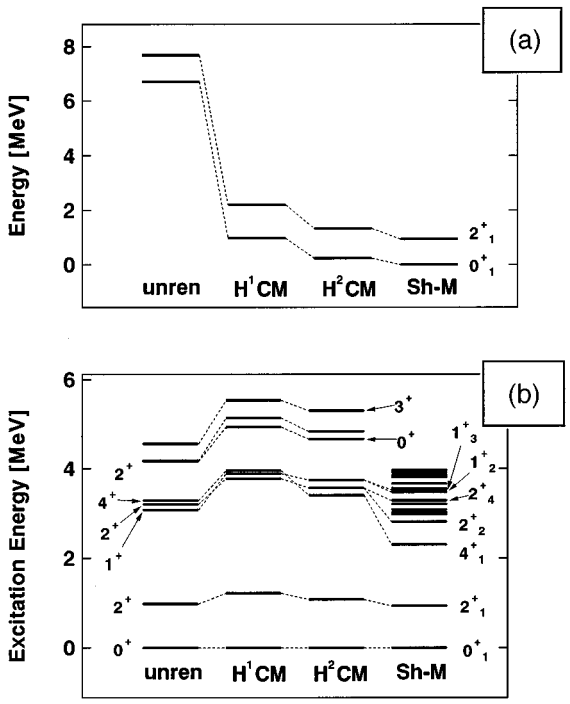

FIG. 1. Energy levels in the collective space (without renormalization, with renormalization via the H^{1}CM, and with renormalization via the H^{2}CM), in comparison with the shell-model ones in ^{56}Fe: (a) lowest 0^+ and 2^+ energy eigenvalues in each space, relative to the shell-model ground-state energy. (b) Energies relative to the lowest 0^+ level in each space.

The H^{n}CM is applied, starting with the collective space composed of these *SD* pairs. The H^{n}CM is driven by the shell-model Hamiltonian in the $k\leqslant 2$ space. The subspace $W_J^{(0)}$ is spanned by the products of the above *SD* pairs with angular momentum J. Any basis in $W^{(0)}$ carries the lowest isospin, and the isospin is conserved during the H^{n}CM. The primary bases $\Psi_\lambda^{(0)}$'s in $W_J^{(0)}$ are put in the order of F spin and seniority, as has been mentioned in the preceding section.

For $n\geqslant 1$, $\Psi_\lambda^{(n)}$'s imply renormalized *SD* states, while they are referred to by the corresponding *SD*-pair structure of $\Psi_\lambda^{(0)}$. Once $\Psi_\lambda^{(n)}$'s are obtained, eigenstates within $W_J^{(n)}$ are calculated by diagonalizing the submatrix of the Hamiltonian whose elements are $\langle\Psi_{\lambda'}^{(n)}|H|\Psi_\lambda^{(n)}\rangle$. In Fig. 1(a), the energies of lowest 0^+ and 2^+ states within the subspace $W^{(n)}$ are shown, in comparison with those of the shell model, for ^{56}Fe. The origin of energy is set to the shell-model ground-state energy. The unrenormalized *SD* states gives far higher energies (the most leftward sector) than the shell-model eigenenergies (the most rightward sector). In this regard, the bare *SD* states (i.e., the primary bases) are insufficient. The renormalization via the H^{n}CM reduces this discrepancy of energies quite efficiently. The H^{2}CM appears to recover the shell-model 0_1^+ and 2_1^+ states satisfactorily well. This observation is confirmed by direct comparison of the wave functions. Table I shows overlaps between the *SD* states and the shell-model eigenstates for the lowest 0^+ and 2^+ states. The unrenormalized states are certainly different from the shell-model eigenstates. A large part of the dis-

TABLE I. Overlaps of wave functions of lowest-lying collective states, before and after the renormalization via the H^2CM, with those of the shell-model eigenstates (%).

Nucleus	0_1^+ Unrenorm.	0_1^+ H^2CM	2_1^+ Unrenorm.	2_1^+ H^2CM
^{56}Fe	55.6	97.0	49.8	93.3
^{54}Cr	53.5	95.8	47.5	92.3
^{58}Fe	46.0	91.2	36.8	83.6
^{56}Cr	54.6	95.1	47.4	90.9

crepancy comes from the $k>0$ configurations. On the contrary, the wave functions after the H^2CM are quite close to the corresponding shell-model ones, having more than 90% overlaps.

Figure 1(b) depicts energy levels for which energies are measured from the ground state defined in each space. It is remarked that the levels without the renormalization resemble the ones after the H^2CM, whereas the H^1CM spectrum is certainly different. The 2_1^+ excitation energy in the original *SD* space is in good agreement with the shell-model result, and therefore with experiments. In the H^1CM result, the 0_1^+ state is greatly lowered owing to the coupling to non-*SD* (i.e., nonprimary) degrees of freedom. Though the 2_1^+ state is also lowered, the non-*SD* effect is smaller than in 0_1^+. Some additional non-*SD* effect is absorbed by the H^2CM, which recovers the 2_1^+ excitation energy. In an analogous manner, as far as the excitation spectra are concerned, the result after the H^2CM is close to the unrenormalized one for most lower-lying states. There is a certain difference in the 1^+ state. We shall return to this point later. The 4_1^+ state appears to be too high, even in the H^2CM result. This state seems to be largely influenced by the *G*-pair degrees of freedom. Although some parts of them are included in the renormalized wave functions, they are not yet sufficient for compensating the whole influence of the *G* pairs.

In Cr nuclei, there is no $|D_\pi^2;0^+\rangle$ basis [i.e., 0^+ state with $(0f_{7/2})^4$ and seniority 4]. It is not always possible, thereby, to create $\Psi_\lambda^{(0)}$ basis having a good *F*-spin value. For instance, the $|0^+(SD^2)\rangle$ bases with good *F* spins are

$$|0^+(SD^2);F=\tfrac{3}{2}\rangle=\frac{1}{\sqrt{3}}(|D_\pi^2;0^+\rangle\otimes|S_\nu\rangle + \sqrt{2}[|S_\pi D_\pi\rangle\otimes|D_\nu\rangle]^{(0)}), \quad (19a)$$

$$|0^+(SD^2);F=\tfrac{1}{2}\rangle=\frac{1}{\sqrt{3}}(\sqrt{2}|D_\pi^2;0^+\rangle\otimes|S_\nu\rangle - [|S_\pi D_\pi\rangle\otimes|D_\nu\rangle]^{(0)}). \quad (19b)$$

Since $|D_\pi^2;0^+\rangle$ does not exist in the present case, only a single $|0^+(SD^2)\rangle$ basis is possible, and we introduce

$$|0^+(SD^2);F=\tfrac{3}{2}\rangle'\equiv[|S_\pi D_\pi\rangle\otimes|D_\nu\rangle]^{(0)}. \quad (20)$$

We replace the higher *F*-spin basis (19a) by Eq. (20). The lower *F*-spin basis is also subject to similar changes, and

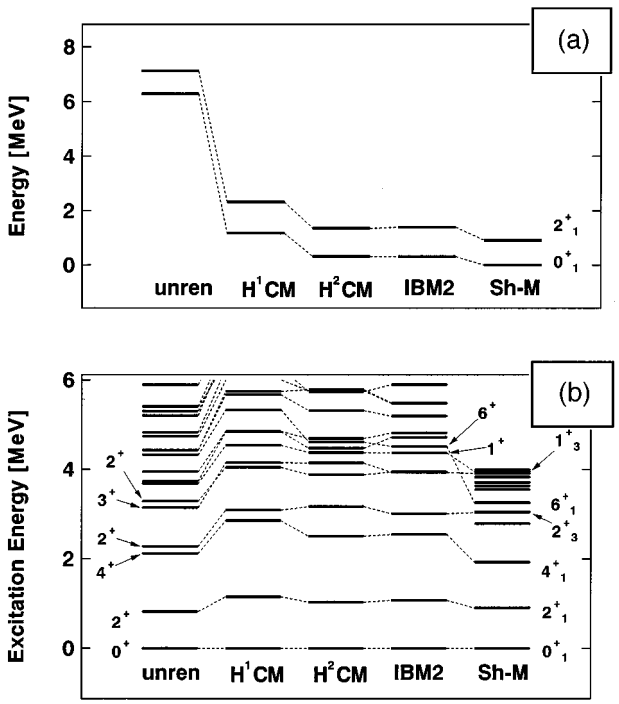

FIG. 2. Energy levels in the collective space compared with the shell-model ones in ^{54}Cr. Energy levels obtained from the IBM-2 Hamiltonian are also shown.

should be modified with proper orthogonalization to the basis assigned with higher *F* value. This orthogonalization, however, annihilates the basis corresponding to Eq. (19b), because of the lack of the $|D_\pi^2;0^+\rangle$ component. The following primary bases are thus obtained:

$$|\Psi_1^{(0)}\rangle=|0^+(S^3);F=\tfrac{3}{2}\rangle, \quad |\Psi_2^{(0)}\rangle=|0^+(SD^2);F=\tfrac{3}{2}\rangle',$$
$$|\Psi_3^{(0)}\rangle=|0^+(D^3);F=\tfrac{3}{2}\rangle. \quad (21)$$

The $|2^+(D^3)\rangle$ bases are handled in an analogous manner. The energy levels in the *SD* space of ^{54}Cr thus constructed are shown in Fig. 2.

For the $N=32$ nuclei, the shell-model energy levels of ^{58}Fe and ^{56}Cr are presented in Figs. 3 and 4, in comparison with the observed ones. This shell-model calculation is performed by using the computer code VECSSE [15]. The $k\leqslant 2$ space leads to the *M*-scheme dimension of 631,670 for ^{58}Fe and 621,478 for ^{56}Cr. Because available experimental data for these nuclei are not as abundant as for the $N=30$ isotones, a stringent assessment of the calculated results appears to be difficult. However, we see that this shell-model calculation reproduces the observed levels reasonably well also for these $N=32$ nuclei.

The structure of neutron *S* and *D* pairs in ^{58}Fe (^{56}Cr) is assumed to be the same as in ^{56}Fe (^{54}Cr), for the sake of simplicity. The $|D_\nu^2;J\rangle$ bases are produced so as to have the generalized seniority [18] of four, by removing lower-seniority components. In ^{56}Cr, the lack of the $|D_\pi^2;0^+\rangle$ component causes a modification of the *SD* bases, as in ^{54}Cr. The energy levels in ^{58}Fe and ^{56}Cr within the *SD* space are shown in Figs. 5 and 6, in comparison with the shell-model ones.

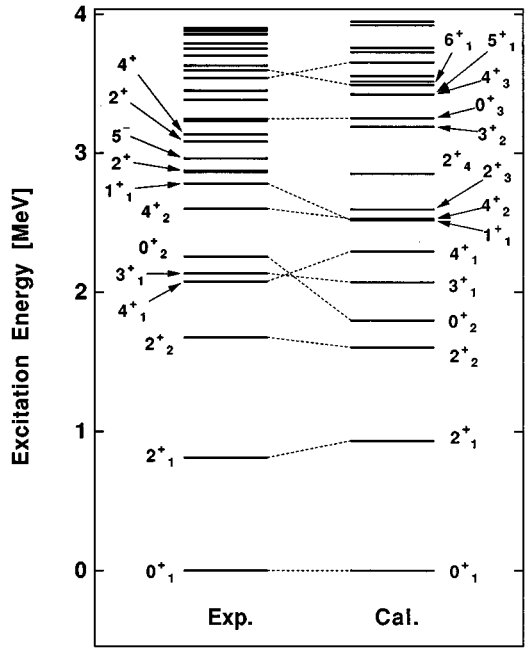

FIG. 3. Energy levels of ^{58}Fe. The experimental data are taken from Ref. [16]. The calculated energy levels are obtained by the $k \leqslant 2$ shell-model calculation with the Kuo-Brown Hamiltonian.

Figures 2, 5, and 6 indicate, respectively, that the H^{2}CM works well for the 0_1^+ and 2_1^+ states of ^{54}Cr, ^{58}Fe, and ^{56}Cr, to the same extent as in ^{56}Fe. As shown in Table I, the wave functions, as well as the energy levels, are in good agreement with the realistic shell-model ones. In ^{54}Cr and ^{56}Cr, the H^{2}CM wave functions have more than 95% overlap with the shell-model eigenstates for 0_1^+, and more than 90% for 2_1^+, as in ^{56}Fe. These numbers are somewhat

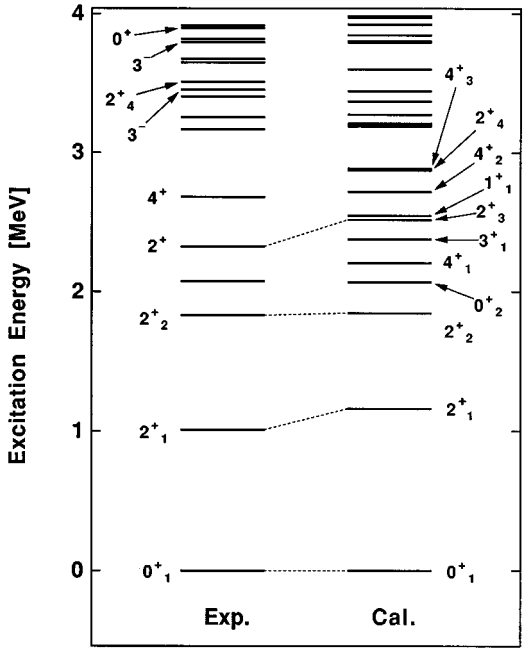

FIG. 4. Energy levels of ^{56}Cr. The experimental data are taken from Ref. [17]. The calculated energy levels are obtained by the $k \leqslant 2$ shell-model calculation with the Kuo-Brown Hamiltonian.

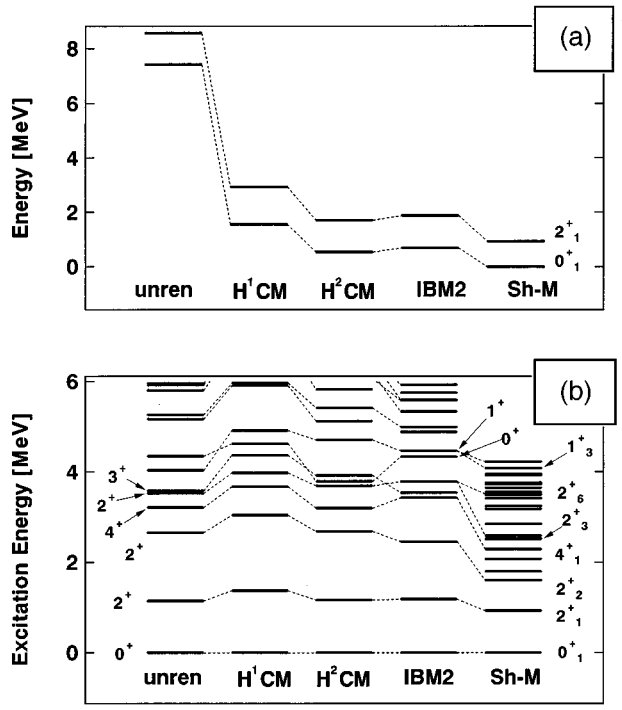

FIG. 5. Energy levels in the collective space, as well as the IBM-2 energy levels, compared with the shell-model ones in ^{58}Fe.

smaller in ^{58}Fe, originating in the smaller overlaps of the unrenormalized *SD* states and the shell-model eigenstates. Though we have presumed the same neutron-pair structure as in ^{56}Fe, a different choice may improve the overlaps. The

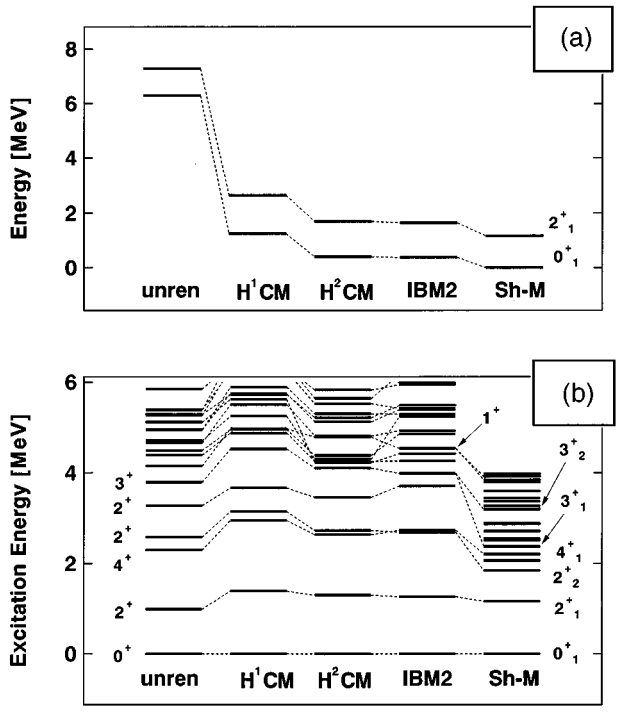

FIG. 6. Energy levels in the collective space, as well as the IBM-2 energy levels, compared with the shell-model ones in ^{56}Cr.

overlaps of the H^{2}CM wave functions with the shell-model ones are still large, exceeding 90% for 0_1^+ and 80% for 2_1^+. Thus the quadrupole collective motion in these nuclei can plausibly be described via the H^{2}CM, based on the realistic shell model.

Although the calculation without the renormalization yields quite high ground-state energy, it produces the energy spectrum similar to that in the H^{2}CM result for most lower-lying states. This consequence is not a trivial one, and seems to give a rather deep insight upon the correspondence between the *SD* pair states and the IBM-2 states.

It should be mentioned here that the renormalization proposed by van Egmond and Allaart [19] has similar aspects to the present one. They have included various correlations induced through a nearly realistic shell-model Hamiltonian. To obtain a renormalized wave function of the state with one *D* pair, the Hamiltonian is diagonalized on the one- and two-broken-pair bases. Most of these bases are involved in the H^{1}CM, if their work is compared with the H^{n}CM. However, a few of them emerge only in H^{2}CM. In this sense, a part of the H^{2}CM effect has been taken into account in Ref. [19]. The H^{n}CM exploited in the present work, on the other hand, provides us with a systematic way to pick up important bases. Wave functions of higher *SD* states are also handled by the H^{n}CM. A significant difference from Ref. [19], as well as from other studies, is that the ^{56}Ni-core excitation plays a certain role in the present case, which may be characteristic to the present mass region. We should note that, because of this point, the $|0^+(S^{N^{\rm B}});F=F_{\rm max}\rangle$ basis is modified to an appreciable extent.

It has been demonstrated how efficient the H^{n}CM is. Despite the relatively heavy leakage out of the *SD* space ($W^{(0)}$), the H^{2}CM yields reasonable energies and wave functions for the lowest-lying states. The leakage mainly arises from the $k>0$ configurations, namely from the ^{56}Ni-core breaking. It is commented that, if we had an appropriate effective interaction in the $k=0$ space, the H^{1}CM, or even the bare *SD* wave functions, might have worked more efficiently.

V. IBM-2 PARAMETERS

We next calculate IBM-2 parameters by extending the OAI mapping, based on the H^{n}CM. There have been numerous investigations devoted to the derivation of the IBM-2 Hamiltonian from schematic interactions like a pairing-plus-quadrupole interaction or a surface-delta interaction [8,9,20]. A semirealistic interaction with the Gaussian form has been applied to investigate several of the IBM-2 parameters in Ref. [19]. On the other hand, this is the first work to derive IBM-2 Hamiltonian from a realistic shell-model interaction; the Kuo-Brown interaction, in the present case.

We employ the following form of the IBM-2 Hamiltonian, including all the possible one- and two-body terms:

$$H^{\rm B}=E_0+\sum_{\rho=\pi,\nu}\epsilon_{d_\rho}\hat{N}_{d_\rho}+\sum_{\rho=\pi,\nu}V_\rho^{\rm B}-\kappa\hat{Q}_\pi\cdot\hat{Q}_\nu+\sum_{J=1,2,3}\xi_J\hat{M}_J+\sum_{J=0,2,4}b_J[d_\pi^\dagger d_\nu^\dagger]^{(J)}\cdot[\tilde{d}_\pi\tilde{d}_\nu]^{(J)}, \tag{22}$$

where

$$\hat{Q}_\rho=[d_\rho^\dagger s_\rho+s_\rho^\dagger\tilde{d}_\rho]^{(2)}+\chi_\rho[d_\rho^\dagger\tilde{d}_\rho]^{(2)}, \tag{23}$$

$$V_\rho^{\rm B}=\frac{1}{2}v_{0,\rho}\{s_\rho^\dagger s_\rho^\dagger\cdot[\tilde{d}_\rho\tilde{d}_\rho]^{(0)}+{\rm H.c.}\}+\frac{1}{\sqrt{2}}v_{2,\rho}\{d_\rho^\dagger s_\rho^\dagger\cdot[\tilde{d}_\rho\tilde{d}_\rho]^{(2)}+{\rm H.c.}\}+\frac{1}{2}\sum_{J=0,2,4}c_{J,\rho}[d_\rho^\dagger d_\rho^\dagger]^{(J)}\cdot[\tilde{d}_\rho\tilde{d}_\rho]^{(J)}. \tag{24}$$

The so-called Majorana terms, which control the energy of the mixed-symmetry states relative to the symmetric states, are defined by

$$\hat{M}_J=[d_\pi^\dagger d_\nu^\dagger]^{(J)}\cdot[\tilde{d}_\nu\tilde{d}_\pi]^{(J)}\quad({\rm for}\ J=1,3), \tag{25a}$$

$$\hat{M}_2=\frac{1}{2}[d_\pi^\dagger s_\nu^\dagger-s_\pi^\dagger d_\nu^\dagger]^{(2)}\cdot[\tilde{d}_\pi s_\nu-s_\pi\tilde{d}_\nu]^{(2)}. \tag{25b}$$

In the OAI mapping, a boson image of a certain nucleon operator is obtained from matrix elements concerning low-seniority states. The parameters are fixed so that a boson matrix element should be equal to the corresponding matrix element in the collective fermion space. We here consider *F* spin also, in addition to the seniority. The boson matrix elements are equated to the fermion ones, similarly to the sequence of the bases in the H^{n}CM discussed in Sec. III. This procedure is briefly illustrated below.

We first consider the *s*-boson condensate $|s^{N^{\rm B}}\rangle$. Since $E_0=(s^{N^{\rm B}}|H^{\rm B}|s^{N^{\rm B}})$, the parameter E_0 in Eq. (22) is fixed by the equation

$$E_0=\langle 0^+(S^{N^{\rm B}});F=F_{\rm max}|H|0^+(S^{N^{\rm B}});F=F_{\rm max}\rangle, \tag{26}$$

where H stands for the shell-model Hamiltonian. When we regard the $|0^+(S^{N^{\rm B}})\rangle$ basis as the unrenormalized one, we obtain the unrenormalized value of E_0 from Eq. (26). By putting the renormalized wave function for $|0^+(S^{N^{\rm B}})\rangle$, the renormalized value of E_0 is evaluated. In this procedure, the wave function renormalization for the collective fermion states gives rise to a renormalization of the IBM-2 parameter. The κ parameter is fixed from the $\langle 0^+(S^{N^{\rm B}})|H|0^+(S^{N^{\rm B}-2}D^2)\rangle$ matrix element. Then ϵ_{d_π} and ϵ_{d_ν} are determined from the following coupled equation:

$$E_0+\frac{1}{N^{\rm B}}(N_\pi^{\rm B}\epsilon_{d_\pi}+N_\nu^{\rm B}\epsilon_{d_\nu})-\frac{2N_\pi^{\rm B}N_\nu^{\rm B}}{N^{\rm B}}\kappa=\langle 2^+(S^{N^{\rm B}-1}D);F=F_{\rm max}|\times H|2^+(S^{N^{\rm B}-1}D);F=F_{\rm max}\rangle, \tag{27a}$$

$$\frac{\sqrt{N_\pi^{\rm B}N_\nu^{\rm B}}}{N^{\rm B}}(N_\pi^{\rm B}\epsilon_{d_\pi}-N_\nu^{\rm B}\epsilon_{d_\nu})+\frac{\sqrt{N_\pi^{\rm B}N_\nu^{\rm B}}(N_\pi^{\rm B}-N_\nu^{\rm B})}{N^{\rm B}}\kappa=\langle 2^+(S^{N^{\rm B}-1}D);F=F_{\rm max}|\times H|2^+(S^{N^{\rm B}-1}D);F=F_{\rm max}-1\rangle. \tag{27b}$$

TABLE II. Parameters for IBM-2 Hamiltonian derived from the Kuo-Brown shell-model Hamiltonian.

Parameter		^{56}Fe		^{54}Cr		^{58}Fe		^{56}Cr	
		Unrenorm.	H^{2}CM	Unrenorm.	H^{2}CM	Unrenorm.	H^{2}CM	Unrenorm.	H^{2}CM
ϵ_{d_π}	(MeV)	1.022	1.362	1.022	1.671	1.022	1.216	1.022	1.591
ϵ_{d_ν}	(MeV)	1.426	1.441	1.482	1.270	1.888	2.004	2.178	2.143
κ	(MeV)	0.839	0.926	0.679	0.765	0.696	0.710	0.558	0.538
χ_π		−0.933	−1.220	0.000	−0.202	−0.933	−1.194	0.000	−0.164
χ_ν		−1.250	−1.099	−1.239	−1.150	−0.005	0.126	0.013	0.205
ξ_1	(MeV)	−0.065	0.303	0.084	0.186	−0.043	0.135	0.080	0.192
ξ_2	(MeV)	0.000	−0.021	0.000	0.127	0.000	0.095	0.000	0.098
ξ_3	(MeV)	−0.009	0.061	0.008	0.171	−0.031	0.198	−0.020	0.152
b_0	(MeV)	0.330	0.575	0.123	−0.099	0.565	0.212	0.337	−0.119
b_2	(MeV)	0.101	0.320	0.034	0.100	0.006	−0.076	−0.001	−0.187
b_4	(MeV)	−0.064	−0.306	−0.104	−0.130	0.003	−0.197	−0.042	−0.030
$v_{2,\pi}$	(MeV)			0.000	0.012			0.000	0.060
$c_{2,\pi}$	(MeV)			0.105	−0.155			0.100	−0.020
$c_{4,\pi}$	(MeV)			−0.424	−1.215			−0.469	−1.033
$v_{0,\nu}$	(MeV)					0.082	0.063	0.141	0.233
$v_{2,\nu}$	(MeV)					−0.441	−0.287	−0.615	−0.690
$c_{0,\nu}$	(MeV)					2.066	1.609	3.399	2.439
$c_{2,\nu}$	(MeV)					−0.308	−1.347	0.053	−0.924
$c_{4,\nu}$	(MeV)					0.447	0.170	0.694	0.593

The other parameters are evaluated in an analogous manner. It should be noticed that in the unrenormalized case this procedure yields the same results as the OAI mapping.

The resultant parameters, the unrenormalized ones and the renormalized ones via the H^{2}CM, are displayed in Table II. For neither ^{56}Fe nor ^{54}Cr, the interaction among neutron bosons (V_ν^{B}) has any effect, since $N_\nu^{\mathrm{B}}=1$. Hence the parameters in V_ν^{B} have not been determined for these nuclei. Likewise, V_π^{B} in the Fe nuclei is not given. For the Cr nuclei, the lack of the $|D_\pi^2;0^+\rangle$ component is realized by setting $c_{0,\pi}=\infty$, while $v_{0,\pi}$ is indeterminate.

It is often assumed, in phenomenological studies, that the IBM-2 Hamiltonian is comprised only of the second, fourth, and fifth terms of Eq. (22). Note that, as far as excitation energies are concerned, the constant term E_0 plays no role. The 2_1^+ excitation energy is governed mainly by the $\hat{N}_d$ and $\hat{Q}_\pi\cdot\hat{Q}_\nu$ terms. For the parameters associated with these terms, the difference between the results with and without the renormalization is not large. For instance, χ_π of the Cr nuclei vanishes before the renormalization, and it remains small after the H^{2}CM. In the $N=32$ nuclei, we have very small χ_ν both in the unrenormalized and H^{2}CM cases. A certain nucleus dependence has been expected for the χ parameters [5]. This variation with the increasing valence nucleon number is rapid in this region, because the size of the shell is small, compared with heavier nuclei.

It is found that, while the Majorana interaction is negligibly small before the renormalization, it becomes sizably repulsive due to the renormalization. In reality, the totally symmetric states are pushed down more than the mixed-symmetry states, absorbing the more effect of non-*SD* degrees of freedom. Thereby the mixed-symmetry states are pushed up to some extent, relative to the lowest-lying states. This point is already viewed in the fermion spectra shown in the preceding section. The repulsive $\hat{M}_1$ term after the H^{2}CM is compatible with increase of the excitation energy of the 1^+ states in Figs. 1, 2, 5, and 6.

It has been shown [8,20] that, if we calculate a boson image of a schematic interaction, the Majorana terms emerge as a renormalization effect. A similar effect occurs also for a realistic interaction derived from the *G* matrix. Nevertheless, there is a difference in mechanism. Whereas only the influence of *g*-boson degree of freedom is considered in Refs. [8,20], various correlation is included in the present renormalization. In particular, the core excitation effect looks to play a certain role in the present case. Energies of the lowest 0^+ and 2^+ (i.e., symmetric) states are lowered greatly, mainly due to the coupling to the core excitation. This mechanism works less for the mixed-symmetry components, resulting in the repulsive Majorana terms.

Comparing the H^{2}CM results on the Majorana terms among the four nuclei, we find certain nucleus dependence of the parameters. In ^{56}Fe, ξ_1 is fairly large with ξ_2 and ξ_3 remaining quite small. The other nuclei have positive values for all of these parameters. The ξ_2 parameter is somewhat smaller than the others.

It is also noticed that V_ρ^{B} and the last term of Eq. (22) are not negligibly small. Though they hardly contribute to the lowest-lying states in these nuclei, some higher-lying states are affected to a certain extent.

By diagonalizing the IBM-2 Hamiltonian, we obtain the energy levels within the IBM-2. They are already displayed in Figs. 1, 2, 5, and 6, by using the parameters after the H^{2}CM. Since we include all the one- and two-body terms in the boson Hamiltonian, the IBM-2 levels in ^{56}Fe, where $N^{\mathrm{B}}=2$, are exactly the same as those of the collective fermion space. In ^{54}Cr, the boson energy levels are very close to those of the collective fermion space, while the perfect

TABLE III. Parameters for IBM-2 transition operators derived from the shell-model operators.

Parameter		^{56}Fe		^{54}Cr		^{58}Fe		^{56}Cr	
		Unrenorm.	H^{2}CM	Unrenorm.	H^{2}CM	Unrenorm.	H^{2}CM	Unrenorm.	H^{2}CM
e_π^{B}	($e$fm^2)	6.635	7.958	5.418	6.563	6.635	7.609	5.418	6.243
e_ν^{B}	($e$fm^2)	6.034	7.273	6.009	6.618	5.057	6.037	5.004	5.365
χ'_π		−0.933	−1.127	0.000	−0.336	−0.993	−1.178	0.000	−0.331
χ'_ν		−1.226	−1.307	−1.205	−1.334	0.011	−0.049	0.035	0.010
g_π^{B}	(μ_N)	1.256	1.110	1.256	1.110	1.256	1.111	1.256	1.110
g_ν^{B}	(μ_N)	−0.027	−0.037	−0.039	−0.080	−0.035	−0.015	−0.038	−0.042
$\beta_{3,\pi}$	($\mu_N$fm^2)	69.1	51.5	69.1	58.4	69.1	51.4	69.1	59.0
$\beta_{3,\nu}$	($\mu_N$fm^2)	−18.8	−20.7	−22.5	−26.3	6.1	8.6	5.3	10.1

agreement can be made if we use three-body terms in the boson Hamiltonian. This indicates that the boson many-body terms are not important. The same holds for ^{58}Fe and ^{56}Cr.

We next turn to electromagnetic transition operators. The following shell-model $E2$ operator is assumed:

$$T(E2)=\sum_{\rho=\pi,\nu} e_\rho^{\mathrm{eff}} \sum_{i\in\rho} r_i^2 Y^{(2)}(\hat{\mathbf{r}}_i), \tag{28}$$

with $e_\pi^{\mathrm{eff}}=1.4e$ and $e_\nu^{\mathrm{eff}}=0.9e$. The single-particle matrix elements are evaluated by the harmonic-oscillator wave functions with $b=56^{1/6}=1.956$ fm. For the $M1$ operator,

$$T(M1)=\sqrt{\frac{3}{4\pi}}\sum_{\rho=\pi,\nu}\left\{g_{l,\rho}^{\mathrm{eff}}\sum_{i\in\rho} l_i+g_{s,\rho}^{\mathrm{eff}}\sum_{i\in\rho} s_i\right\}, \tag{29}$$

and we take $g_{l,\rho}^{\mathrm{eff}}=g_{l,\rho}^{\mathrm{free}}$, $g_{s,\rho}^{\mathrm{eff}}=0.5g_{s,\rho}^{\mathrm{free}}$. These electromagnetic operators are the same as in Ref. [1]. While medium effect on the $M3$ operator has not been explored sufficiently, there is an evidence in the sd shell that no quenching is necessary to describe $M3$ transitions [21]. The shell-model $M3$ operator is taken to be equal to the bare-nucleon operator,

$$T(M3)=\frac{\sqrt{21}}{2}\sum_{\rho=\pi,\nu}\left\{g_{l,\rho}^{\mathrm{free}}\sum_{i\in\rho} r_i^2[Y^{(2)}(\hat{\mathbf{r}}_i)l_i]^{(3)} +2g_{s,\rho}^{\mathrm{free}}\sum_{i\in\rho} r_i^2[Y^{(2)}(\hat{\mathbf{r}}_i)s_i]^{(3)}\right\}, \tag{30}$$

where the g parameter are the same as for the free $M1$ operator.

The IBM-2 operators are

$$T^{\mathrm{B}}(E2)=\sum_{\rho=\pi,\nu} e_\rho^{\mathrm{B}}\{[d_\rho^\dagger s_\rho+s_\rho^\dagger\tilde{d}_\rho]^{(2)}+\chi'_\rho[d_\rho^\dagger\tilde{d}_\rho]^{(2)}\}, \tag{31}$$

$$T^{\mathrm{B}}(M1)=\sqrt{\frac{3}{4\pi}}\sum_{\rho=\pi,\nu} g_\rho^{\mathrm{B}}\hat{J}_\rho^{\mathrm{B}};\quad \hat{J}_\rho^{\mathrm{B}}=\sqrt{10}[d_\rho^\dagger\tilde{d}_\rho]^{(1)}, \tag{32}$$

$$T^{\mathrm{B}}(M3)=\sum_{\rho=\pi,\nu}\beta_{3,\rho}[d_\rho^\dagger\tilde{d}_\rho]^{(3)}. \tag{33}$$

The parameters introduced above are evaluated from the matrix elements within the collective fermion space, analogously to the mapping for the Hamiltonian. The resultant IBM-2 parameters are shown in Table III.

The renormalization enhances the boson effective charges (e_ρ^{B}), gaining more quadrupole collectivity. In phenomenological studies, $e_\pi^{\mathrm{B}}=e_\nu^{\mathrm{B}}$ is sometimes postulated. This is supported by the present microscopic study. Though the shell-model effective charge is smaller for neutrons than for protons, the neutrons have more quadrupole collectivity because the size of the valence shell is bigger. As a consequence, e_π^{B} and e_ν^{B} are not so different. There is no apparent reason for the χ' parameters to agree with the χ parameters which appear in the boson Hamiltonian, because we adopt a realistic shell-model interaction, not a schematic proton-neutron interaction like $Q_\pi\cdot Q_\nu$. Nevertheless, χ' is close to χ in any case. It has been expected that $g_\pi^{\mathrm{B}}\simeq g_{l,\pi}^{\mathrm{free}}=1$ and $g_\nu^{\mathrm{B}}\simeq g_{l,\nu}^{\mathrm{free}}=0$, since the nucleon-spin degrees of freedom are not so active in the quadrupole collective states. However, g_π^{B} is certainly larger than unity in the result without the renormalization. This happens because the proton SD pairs consist of the single-j orbit of $0f_{7/2}$. On the contrary, when we carry out the renormalization, the excitation from $0f_{7/2}$ to $0f_{5/2}$ leads towards saturation of the nucleon spin. Therefore the g_π^{B} value is reduced until $g_\pi^{\mathrm{B}}\simeq 1$ is restored to a good extent. The quenching of $\beta_{3,\pi}$ due to the renormalization is explained by a similar spin-saturation mechanism. It is somewhat surprising that the influence of the renormalization on g_ν^{B} and $\beta_{3,\nu}$ is so small. This will be partly because the spin saturation occurs already in the unrenormalized neutron parameters, resulting in almost vanishing values.

The same quenching mechanism for the magnetic transition parameters will prevail in heavier nuclei, where a unique-parity orbit is involved in the valence shell. Since the spin-orbit partner of the unique-parity orbit is absent in the valence shell, the nucleon-spin content could influence g_ρ^{B} and $\beta_{3,\rho}$ to a considerable extent, when we ignore effects of excitation across major shells. However, by taking into account the excitation effects, those parameters will be quenched, owing to the spin-saturation tendency [22] in the dynamics. It is expected for the $M1$ parameters that g_π^{B} approaches unity and g_ν^{B} almost vanishes.

The dependence of the IBM-2 parameters on valence nucleon numbers is accounted for, in most cases, in terms of

the quasispin properties of the relevant nucleon operator [5]. The $E2$ operator behaves as a vector in the quasispin space [23]. Weak dependence is suggested for $e_\rho^{\rm B}$ and is confirmed in Table III. The number dependence of χ' is strong, as is expected. So is χ in the boson Hamiltonian. Since $T(M1)$ and $T(M3)$ are quasispin scalars [23], the $g_\rho^{\rm B}$ and $\beta_{3,\rho}$ parameters are expected to be nearly constant. This is true for $g_\pi^{\rm B}$, $g_\nu^{\rm B}$, and $\beta_{3,\pi}$, but a considerable deviation is seen in $\beta_{3,\nu}$. This is a sort of many-body effect, originating in the subshell structure.

VI. DISCUSSION ON H^{n}CM

A. Choice of primary bases

In this section, we return to discussion on the H^{n}CM.

Even when the subspace $W_J^{(0)}$ is fixed, there still remains an ambiguity in choosing the primary orthonormal bases $\{\Psi_1^{(0)},\Psi_2^{(0)},\ldots,\Psi_l^{(0)}\}$. The bases can be changed by a unitary transformation. Since the couplings between $\phi_\lambda^{(\nu-1)}$ and $\phi_\lambda^{(\nu)}$ are not uniform for various λ, the unitary transformation may lead to a different renormalized basis set in the H^{n}CM. Moreover, because of the orthogonalization stated in Sec. III, the H^{n}CM bases generally depends on the ordering of the primary bases.

The following three choices will be possible.

(i) Some orthonormal basis set is postulated for $\Psi_\lambda^{(0)}$ by a physical insight.

(ii) The eigenstates within $W_J^{(0)}$ are taken as $\Psi_\lambda^{(0)}$. They are placed in order according to the eigenenergies.

(iii) $\Psi_\lambda^{(0)}$ is redefined for each step n, so that $\Psi_\lambda^{(n-1)}$ should be an eigenstate within $W_J^{(n-1)}$. They are put in order according to the eigenenergies.

To fulfill the space closure of Eq. (4), the couplings between renormalized states and remaining degrees of freedom should be small. From this viewpoint, the latter choice seems favorable. On the other hand, the latter requires more complication in the numerical treatment.

The basic dynamical properties should be well represented by the primary bases, otherwise the renormalization does not converge with small n. In the practical case of the Cr-Fe nuclei in Secs. III and IV, we have adopted (i), with the $\mathrm{U}_{\pi+\nu}(5)\otimes\mathrm{SU}_F(2)$ bases of IBM-2 [24]. This will be appropriate because those nuclei seem to be nearly spherical. In deformed region, another choice might be better [25].

B. Choice of renormalized bases

One could pursue the convergence of H^{n}CM, by increasing the power n. However, besides tedious computations, it might lead to a dissimilar wave function of $\Psi_\lambda^{(n)}$ from that of $\Psi_\lambda^{(0)}$. Then it is not reasonable to regard $\Psi_\lambda^{(n)}$ as a renormalized state. In some cases, this is circumvented if an eigenstate in $\Gamma_\lambda^{(n)}$ having the largest overlap with $\Psi_\lambda^{(0)}$ is adopted as $\Psi_\lambda^{(n)}$, instead of the lowest-lying one.

A complication occurs when there is a substantial fragmentation of the state which carries the main character of the primary state. As has been pointed out in Ref. [1], the mixed-symmetry 2^+ state of ^{56}Fe may be the case. The 2_2^+ and 2_4^+ states share appreciable fractions of this collective component. As n increases, the diagonalization within $\Gamma_\lambda^{(n)}$ will lead to a problem at some value of n; plural eigenstates have considerable amplitudes of the primary basis $\Psi_\lambda^{(0)}$. It will not be desirable, in such a case, to choose a single eigenstate in $\Gamma_\lambda^{(n)}$ as a renormalized basis $\Psi_\lambda^{(n)}$.

A solution to this problem is to adopt a linear combination of the few eigenstates in $\Gamma_\lambda^{(n)}$ as a renormalized basis. We can set a criterion of minimum amplitude for the states to be included. Another practical choice is just stopping at a certain n. It should be emphasized that, in any case, monitoring the H^{n}CM outcome for each step is significant.

In the actual case of the Cr-Fe nuclei, we do not come across the problems stated above, up to the H^{2}CM. The lowest-lying eigenstate in $\Gamma_\lambda^{(n)}$ has the largest overlap with $\Psi_\lambda^{(0)}$, and no serious fragmentation is viewed. As shown in Sec. IV, the convergence in 0_1^+ and 2_1^+ is so rapid that we could acquire a good approximation by the H^{2}CM. In this respect, the H^{2}CM seems good enough to investigate collective states of the Cr-Fe nuclei.

C. H^{n}CM and Lanczos method

As has been mentioned earlier, there is a common part between the H^{n}CM and the Lanczos diagonalization method.

The H^{n}CM energy levels are obtained via two steps of diagonalization; one within the subspace $\Gamma_\lambda^{(n)}$ and the other within $W_J^{(n)}$. The dimension of $\Gamma_\lambda^{(n)}$ is $(n+1)$, while that of $W_J^{(n)}$ is l. The basis production and the diagonalization within $\Gamma_\lambda^{(n)}$ is similar to the Lanczos method. In the case that there is a single basis in $W_J^{(0)}$, the H^{n}CM procedure is the same as the Lanczos method starting from $\Psi^{(0)}$, since we do not need the diagonalization within $W_J^{(n)}$. In other cases, the orthogonalization between $\Gamma_\lambda^{(n)}$ and $\Gamma_{\lambda'}^{(n)}$ $(\lambda\neq\lambda')$ in the H^{n}CM does not appear in the Lanczos method. Apart from this difference, the H^{n}CM is exploited so as to make good use of the advantage of the Lanczos method.

An emphasis should be put on the primary bases: we have requested that they should have a simple structure but carry the basic dynamics of the system. For instance, the SD states are taken as the primary bases in the application to the Cr-Fe nuclei in Sec. IV. Because of these properties, it is expected in many cases that the H^{n}CM is more efficient than the Lanczos method. The number of bases in the H^{n}CM is given by $l(n+1)$ for each J, which can be smaller than that necessary in the Lanczos method. In practice, within a fixed J, even less than 10 bases yield good accuracy for the lowest-lying levels of the Cr-Fe nuclei via the H^{n}CM, whereas about 50 bases are normally required in the Lanczos method. It is noted that each diagonalization is performed for a matrix with quite a small dimension, $(n+1)$ or l.

D. H^{n}CM and a perturbative renormalization

In this subsection, the H^{n}CM is discussed in connection with a perturbative method of renormalization. A more detailed discussion is given in Ref. [2].

Let us recall Feshbach's projection method [10], a well-known method of incorporating truncation effects. We define the P space as the space of the primary bases; the original SD space in the present case. The total space corresponds to

the $k \leqslant 2$ shell-model space, while the original Hamiltonian is the Kuo-Brown Hamiltonian. We shall take into account the effects of the Q space, which is spanned by the nonprimary bases. Note that all the ϕ bases of Eq. (8) belong to the Q space. The projection operator onto the P space is denoted by $\hat{P}$, and that onto the Q space by $\hat{Q}$, namely $\hat{Q}=1-\hat{P}$.

In Feshbach's method, the renormalized P space Hamiltonian is given by

$$\widetilde{H}_P = H_P + \hat{P}H\hat{Q}\frac{1}{E-H_Q}\hat{Q}H\hat{P}, \tag{34}$$

where

$$H_P = \hat{P}H\hat{P}, \quad H_Q = \hat{Q}H\hat{Q}. \tag{35}$$

For the exact treatment of H_Q, eigenvalues of H_Q have to be calculated. Let an eigenstate of H_Q be denoted by $|q_i\rangle$. Notice that $\hat{Q}|q_i\rangle = |q_i\rangle$ and $\hat{Q} = \Sigma_i |q_i\rangle\langle q_i|$. Then the second term on the right-hand side of Eq. (34) is rewritten as

$$\sum_i \hat{P}H|q_i\rangle \frac{1}{E-E(q_i)}\langle q_i|H\hat{P}, \tag{36}$$

where $E(q_i)=\langle q_i|H|q_i\rangle$. Though Eq. (34) gives an exact way to incorporate the influence of the Q space into the Hamiltonian, it is difficult and not advantageous to handle without any approximation in most cases, because of the following two reasons. If one wishes to know exact eigenenergies, H_Q must be treated exactly, which is usually a matrix with enormous dimension. Moreover, a nonlinear coupled equation must be solved, since the eigenenergy E is also contained in the denominator of the second term.

For the sake of simplicity, our discussion is restricted to a fixed J (conserved quantum number), without loss of generality. We introduce the following state generated from $\Psi_\lambda^{(0)}$:

$$|\overline{\phi_\lambda}\rangle = \sum_i x_{i,\lambda}|q_i\rangle \propto \hat{Q}H|\Psi_\lambda^{(0)}\rangle \quad (\lambda = 1,2,\ldots,l), \tag{37}$$

where

$$x_{i,\lambda} = \frac{\langle q_i|H|\Psi_\lambda^{(0)}\rangle}{\sqrt{\Sigma_{i'}|\langle q_{i'}|H|\Psi_\lambda^{(0)}\rangle|^2}} = \frac{\langle q_i|H|\Psi_\lambda^{(0)}\rangle}{\sqrt{\langle\Psi_\lambda^{(0)}|H\hat{Q}H|\Psi_\lambda^{(0)}\rangle}}. \tag{38}$$

It is noticed that, with the notation in Sec. III, $\overline{\phi_\lambda}$ can be expressed as $P^{\mathcal{O}}_{\{\Psi_1^{(0)},\Psi_2^{(0)},\cdots,\Psi_l^{(0)}\}}\cdot H\Psi_\lambda^{(0)}$ which is different from the basis $\phi_\lambda^{(1)}$ only in the lack of orthogonalization between ϕ_λ and $\phi_{\lambda'}$ $(\lambda \neq \lambda')$.

We now substitute a c number $E(\overline{\phi_\lambda}) = \langle\overline{\phi_\lambda}|H|\overline{\phi_\lambda}\rangle$ for H_Q in Eq. (34). Then a diagonal matrix element of $\widetilde{H}_P$ is approximated by

$$\begin{aligned}\langle\Psi_\lambda^{(0)}|\widetilde{H}_P|\Psi_\lambda^{(0)}\rangle &\simeq \langle\Psi_\lambda^{(0)}|H|\Psi_\lambda^{(0)}\rangle \\ &\quad + \langle\Psi_\lambda^{(0)}|H|\overline{\phi_\lambda}\rangle\frac{1}{E-E(\overline{\phi_\lambda})}\langle\overline{\phi_\lambda}|H|\Psi_\lambda^{(0)}\rangle \\ &= \langle\Psi_\lambda^{(0)}|H|\Psi_\lambda^{(0)}\rangle \\ &\quad + \frac{1}{E-E(\overline{\phi_\lambda})}\langle\Psi_\lambda^{(0)}|H\hat{Q}H|\Psi_\lambda^{(0)}\rangle. \end{aligned} \tag{39}$$

This is a kind of closure approximation, since it is given by replacing the energy denominator by a c number. It is not easy, in general, to evaluate E in the energy denominator properly. By substituting unperturbed energy $E_\lambda^{(0)} = \langle\Psi_\lambda^{(0)}|H|\Psi_\lambda^{(0)}\rangle$ for it, Eq. (39) becomes equivalent to the second-order perturbation combined with the closure approximation. It is remarked that, however, the unperturbed energy is too high in the practical case of the Cr-Fe nuclei, causing too big a renormalization effect. If we neglect the nonorthogonality between ϕ_λ and $\phi_{\lambda'}$ for $\lambda \neq \lambda'$, the space $\Gamma_\lambda^{(1)}$ becomes $\{\Psi_\lambda^{(0)}, \phi_\lambda\}$. In addition, if E is estimated by diagonalizing the Hamiltonian in this $\Gamma_\lambda^{(1)}$ space, we obtain $E_\lambda^{(1)}$. Then the right-hand side of Eq. (39) is equivalent to the diagonal element of the H^{1}CM collective Hamiltonian. Note that $E_\lambda^{(1)}$ is lower than $E_\lambda^{(0)}$, and is closer to the exact E for low-lying states.

Observing the above relation between the H^{1}CM and the perturbative renormalization with closure approximation, we can claim that the H^{1}CM is an improvement from the perturbative method in the following points: (i) the overcounting arising from the non-orthogonality between ϕ_λ and $\phi_{\lambda'}$ $(\lambda \neq \lambda')$ is removed, (ii) off-diagonal elements are evaluated in a consistent manner with diagonal ones, and (iii) E in the energy denominator is improved. If the overlap between ϕ_λ and $\phi_{\lambda'}$ is negligible, which somewhat depends on how to choose the original basis set $\{\Psi_\lambda^{(0)}; \lambda = 1,2,\ldots,l\}$, ϕ_λ and $\phi_\lambda^{(1)}$ becomes quite similar. In order to further make the relationship between the two methods more transparent, we shall restrict ourselves to the diagonal elements and ignore how E is estimated.

If the second term of the right-hand side of Eq. (34) is expanded by the parameter

$$\zeta_{i,\lambda} = \frac{E(\overline{\phi_\lambda}) - E(q_i)}{E-E(\overline{\phi_\lambda})}, \tag{40}$$

we obtain [2]

$$\begin{aligned}&\left\langle \Psi_\lambda^{(0)}\middle|\hat{P}H\hat{Q}\frac{1}{E-H_Q}\hat{Q}H\hat{P}\middle|\Psi_\lambda^{(0)}\right\rangle \\ &\quad = \frac{1}{E-E(\overline{\phi_\lambda})}\langle\Psi_\lambda^{(0)}|H\hat{Q}H|\Psi_\lambda^{(0)}\rangle\left\{1+\left[\frac{\sigma_\lambda(H_Q)}{E-E(\overline{\phi_\lambda})}\right]^2\right\} \\ &\quad + O(\zeta^3), \end{aligned} \tag{41}$$

where

$$[\sigma_\lambda(H_Q)]^2 = \langle\overline{\phi_\lambda}|H_Q^2|\overline{\phi_\lambda}\rangle - [E(\overline{\phi_\lambda})]^2 \tag{42}$$

represents variance of H_Q in the state $\overline{\phi_\lambda}$. In a similar manner, the $O(\zeta^n)$ term corresponds to correction due to the nth moment of the distribution of $|q_i\rangle$'s. By comparing Eq. (41) with Eq. (39), it is found in $O(\zeta^2)$ that the distribution of $\overline{\phi_\lambda}$ over the eigenstates of H_Q generally enhances the effect of the renormalization on energies.

The above discussion is useful to acquire an intuitive picture of the H^{n}CM. The terms regarding H_Q^2 are fully taken into account in the H^{2}CM. Therefore, as far as diagonal elements are concerned, the difference between Eq. (41) and the H^{2}CM is only in $O(\zeta^3)$. In comparison with the H^{1}CM, an advantage of the H^{2}CM is the inclusion of the $O(\zeta^2)$ effect [2]. As stated already, in the perturbative theory, which is connected to the H^{1}CM well, the coupling of a primary state with the outer space (Q space) is treated by using an averaged energy of the nonprimary states $E(\overline{\phi_\lambda})$, ignoring their distribution. The second-order effect is, in essence, the correction due to the distribution of the coupled states in terms of the variance, as shown in Eq. (41). By extending the present discussion to higher order, it turns out that the nth order effect of H^{n}CM essentially corresponds to the nth moment of the distribution of $\overline{\phi_\lambda}$ in the Q space.

We now look back at the results shown in Figs. 1, 2, 5, and 6 in Sec. IV. In proceeding from H^{1}CM to H^{2}CM, the higher-lying states tend to go down more sharply. This implies that the variance $\sigma_\lambda(H_Q)$ is more important in the higher-lying state. On the other hand, some mixed-symmetry states with relatively low energy (for instance, the lowest 1^+ and the second 2^+ states in the collective space of each nucleus) do not come down so rapidly, compared with their surrounding states. Relatively small $\sigma_\lambda(H_Q)$ is suggested for those mixed-symmetry degrees of freedom, giving rise to the repulsive Majorana interaction in the IBM-2 Hamiltonian.

VII. SUMMARY

In order to study quadrupole collective modes based on a realistic shell model, we develop the H^n-cooling method (H^{n}CM), which leads to a wave function renormalization by incorporating the effect of the dynamical correlation. In practice, the H^{n}CM is applied to the SD space of the Cr-Fe nuclei: ^{56}Fe, ^{54}Cr, ^{58}Fe, and ^{56}Cr. While the shell-model ground-state wave function is not fully covered with the simple SD pair degrees of freedom, the shell-model 0_1^+ and 2_1^+ energies and wave functions are nicely approximated by considering up to the second power of H (H^{2}CM). On the other hand, as far as the energy difference is concerned, the excitation spectra after the H^{2}CM do not differ very much from those without the renormalization. Note that the ^{56}Ni-core excitation is taken into account in the present renormalization, as well as some effect of other like-nucleon pairs.

An extended OAI mapping is also developed and applied to the Cr-Fe nuclei. This is the first work to evaluate the IBM-2 parameters from a realistic shell-model Hamiltonian. The wave function renormalization is converted to a renormalization of the IBM-2 parameters. Some effects of the renormalization are discussed. Although most parameters in the IBM-2 Hamiltonian do not change considerably, the Majorana interaction becomes sizably repulsive as a renormalization effect. It is indicated that many-body terms are unnecessary in the IBM-2 Hamiltonian. In the transition operators, the H^{n}CM gives rise to spin quenching for the $M1$ and $M3$ proton parameters, as well as $E2$ effective-charge enhancement. The χ parameters in the $E2$ operator are shown to take close values to those in the Hamiltonian. This situation is not influenced by the renormalization.

ACKNOWLEDGMENTS

The authors are grateful to Professor A. Gelberg for careful reading of the manuscript. One of the authors (H.N.) thanks Professor T. Sebe for his advice on the computer programs.

[1] H. Nakada, T. Otsuka, and T. Sebe, Phys. Rev. Lett. **67**, 1086 (1991); in *Capture Gamma-Ray Spectroscopy*, edited by R. W. Hoff, AIP Conf. Proc. No. 238 (American Institute of Physics, New York, 1991), p. 131.
[2] H. Nakada, Ph.D. thesis, University of Tokyo, 1991.
[3] H. Nakada, T. Sebe, and T. Otsuka, Nucl. Phys. **A571**, 467 (1994); H. Nakada, in *Proceedings of International Symposium on Frontier of Nuclear Structure Physics*, edited by M. Ishihara *et al.* (World Scientific, Singapore, 1996), p. 15.
[4] T. T. S. Kuo and G. E. Brown, Nucl. Phys. **A114**, 241 (1968).
[5] T. Otsuka, A. Arima, and F. Iachello, Nucl. Phys. **A309**, 1 (1978); T. Otsuka, in *Algebraic Approaches to Nuclear Structure*, edited by R. F. Casten (Harwood Academic Publishers, Chur, 1993), p. 195.
[6] F. Iachello, Nucl. Phys. **A358**, 89c (1981); A. E. L. Dieperink, Prog. Part. Nucl. Phys. **9**, 121 (1983).
[7] S. A. A. Eid, W. D. Hamilton, and J. P. Elliott, Phys. Lett. **166B**, 267 (1986); S. P. Collins *et al.*, J. Phys. G **15**, 321 (1989); K. P. Lieb *et al.*, Phys. Lett. B **215**, 50 (1988).
[8] C. H. Druce, S. Pittel, B. R. Barrett, and P. D. Duval, Ann. Phys. (N.Y.) **176**, 114 (1987).
[9] T. Mizusaki, Ph.D. thesis, University of Tokyo, 1992.
[10] H. Feshbach, Ann. Phys. (N.Y.) **19**, 287 (1962).
[11] T. T. S. Kuo and E. Osnes, *Folded Diagram Theory of the Effective Interaction in Nuclei, Atoms and Molecules*, Lecture Notes in Physics Vol. 364 (Springer-Verlag, Berlin, 1990).
[12] H. Horie and T. Ogawa, Prog. Theor. Phys. **46**, 439 (1971); Nucl. Phys. **A216**, 407 (1973).
[13] P. Halse, Phys. Rev. C **41**, 2340 (1990); **44**, 2467 (1991).
[14] H. Nakada and T. Otsuka, submitted to Phys. Rev. C.
[15] T. Sebe, Y. Shikata, T. Otsuka, H. Nakada, and N. Fukunishi, VECSSE, Program library of Computer Centre, University of Tokyo (1994).
[16] L. K. Peker, Nucl. Data Sheets **61**, 189 (1990).
[17] H. Junde *et al.*, Nucl. Data Sheets **67**, 523 (1992).
[18] I. Talmi, Nucl. Phys. **A172**, 1 (1971).
[19] A. van Egmond and K. Allaart, Phys. Lett. **131B**, 275 (1983); Nucl. Phys. **A425**, 275 (1984).

[20] O. Scholten, Phys. Rev. C **28**, 1783 (1983).
[21] K. K. Seth *et al.*, Phys. Rev. Lett. **74**, 642 (1995); **74**, 3306 (1995).
[22] A. Arima, K. Shimizu, W. Bentz, and H. Hyuga, in *Advances in Nuclear Physics*, edited by J. W. Negele and E. Vogt (Plenum Press, New York, 1988), Vol. 18, p. 1.
[23] A. Arima and M. Ichimura, Prog. Theor. Phys. **36**, 296 (1966).
[24] F. Iachello and A. Arima, *The Interacting Boson Model* (Cambridge University Press, Cambridge, 1987).
[25] N. Yoshinaga, in *Proceedings of International Conference: Perspectives for the Interacting Boson Model on the Occasion of its 20th Anniversary*, edited by R. F. Casten *et al.* (World Scientific, Singapore, 1994), p. 213.